PMM U.S.S.R.,Vol.47,No.3,pp.376-382,1984
Printed in Great Britain

0021-8928/84 $10.00+0.00

UDC 532.546.06

PROBLEM OF FILTRATION FROM A SYSTEM OF CHANNELS AT THE BORDER ZONE SEPARATING FRESH WATERS FROM SALINE WATERS LYING BELOW, WITH EVAPORATION*

E.N. BERESLAVSKII and V.N. EMIKH

Methods of the analytic theory of linear differential equations are used to solve the problem of steady filtration from a system of channels in a boundary separating fresh water from saline water lying below it, with evaporation given in the form of a linear dependence of the stream function on the abscissa. A sequential computational algorithm based on the solution, is given. It is explained that the system of flow in question can be realized only in the case when the initial depth of the saline water exceeds a certain value dependent on the remaining initial parameters at which the boundary degenerates into a chain of lenses. Such a minimum depth admissible in the border zone scheme is found in every variant by preliminary computation of the lens using a previously obtained analytic solution of the corresponding problem /1/; the problem itself is solved in /2/ for the general linear law of evaporation.

1. Formulation of the problem. A plane, steady state filtration takes place in a fresh water border zone formed in a homogeneous layer of soil above stagnant saline water from a system of periodically distributed channels with rectilinear contours with profiles of width $2l$, and low depth of water. The influx of water into the border zone is compensated by its evaporation from the free surface. Neglecting the thickness of the transition zone, we shall follow an approach adopted in problem of this type /1- 3/ and begin with the fact that a boundary line exists separating fresh water from the saline water. Fig.1 depicts schematically one of the half-periods of the flow (region z); the depression curve BC and separation line ED are to be determined. The following conditions hold along the boundary of the region z:

$$\begin{aligned} &AB: y = 0,\ \varphi = 0;\ AE: x = 0,\ \psi = 0;\ CD: x = L, \psi, = 0 \\ &ED: \varphi - \rho y = C_0 = \text{const},\ \psi = 0\ \ (\rho = \rho_2 / \rho_1 - 1) \\ &BC: \varphi + y = 0,\ \psi = \varepsilon (L - x) \end{aligned} \tag{1.1}$$

Here φ and ψ are self-conjugate functions harmonic within the region z and representing the filtration rate potential and stream function relative to the soil filtration coefficient, L is half-distance between the centers of adjacent channels, ρ_1 and ρ_2 are the densities of the fresh and saline water and $(\rho_2 > \rho_1)$. The first relation of (1.1) for the segment ED comes from the assumption that the saline water is stagnant and that the pressure remains continuous during the passage across the boundary line /3/. According to the last relation of (1.1) the amount evaporated from a certain segment of the depression curve is proportional to the length of the horizontal projection of this segment /1/.

The quantities $L, l, \varepsilon, \rho,$ serve, subject to the conditions

$$0 < l < L,\ 0 < \varepsilon < \rho,\ \varepsilon (L - l) < l \tag{1.2}$$

as the physical defining parameters, together with the depth H_0 of the initial (prior to formation of border) surface of the saline ground water. If the latter, being incompressible, is isolated from sources and sinks, then their displacement under the channels must be compensated by their rise between the channels without change in volume, and this yields the relation (Fig.1)

$$\int_0^L [y_{ED}(x) + H_0]\, dx = 0 \tag{1.3}$$

Below we shall explain that in this approach the quantity H_0 is bounded from below by some value H_{00} depending on L, l, ε and ρ. When $H_0 < H_{00}$, the border decomposes into separate lenses. The last inequality of (1.2) means that, in the presence of backwater effect, the

*Prikl.Matem.Mekhan.,Vol.47.No.3,pp.446-454,1983 reduced filtration discharge from the channel equal, under the conditions of steady state flow to total evaporation $\varepsilon(L-l)$ from the free surface of the border, must not exceed the flow rate l of the unrestricted filtration.

We shall mention another possible variant of the formulation under which the border is underlayed with mineralized water bound to a strongly permeable level lying below it and acted upon by a some constant (by virtue of its immobility) piezometric pressure h. In this case the first condition of (1.1) on the segment ED written e.g. for the point E, yields directly (see also /3/, ch.VIII, formula (10.2))

$$\varphi_E - \rho y_E = (\rho_2/\rho_1)\, h$$

The expressions for quantities φ_E, y_E are the same as for $y_{ED}(x)$ in (1.3) are obtained from the solution of the problem.

2. Constructing the solution.

For the flow scheme in question the segments (or their continuations) of the boundary of the velocity hodograph $\overline{W} = W_x + iW_y$ shown in Fig.2 have no common point, and this prevents us from solving the problem by known methods of conformal mapping /4/. We shall therefore use the P.Ia. Polubarinova-Kochina method based in the application of the analytic theory of linear differential equations (/3/, ch.VII). We introduce the functions $z(\zeta)$ and $\omega(\zeta)$, which map conformally the regions $z = x + iy$ and $\omega = \varphi + i\psi$ onto the half-plane $\operatorname{Im}\zeta \geqslant 0$ of the auxilliary complex variable ζ (Fig.3a) and are to be determined. The functions

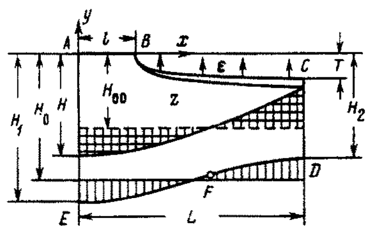

Fig.1

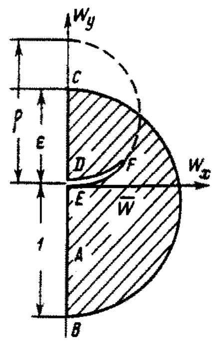

Fig.2

$$Z(\zeta) = dz/d\zeta, \qquad \Omega(\zeta) = d\omega/d\zeta \tag{2.1}$$

represent solutions of certain second order linear differential Fuchsian equation with regular singularities represented by the singularities of the functions z and ω. The general integral $Y(\zeta)$ of this equation can be represented by the following Riemann symbol containing the indices at the singularities:

$$Y(\zeta) = P\begin{Bmatrix} a_0 & 0 & f_0 & 1 & 1/k^2 & \infty & \\ -{}^1/_2 & 0 & 0 & 0 & 0 & {}^3/_2 & \zeta \\ -{}^1/_2 & -{}^1/_2 & 2 & -{}^1/_2 & -{}^1/_2 & 2 & \end{Bmatrix} \tag{2.2}$$

We pass to the function $Y^\circ(\zeta)$ using the transformation

$$Y(\zeta) = Y^\circ(\zeta)/[2\sqrt{(\zeta-a_0)\zeta(1-\zeta)(1-k^2\zeta)}] \tag{2.3}$$

and we eliminate during the passage the removable singularity A.

The differential equation the general integral of which is represented by the function $Y^\circ(\zeta)$, has the form /5/

$$\frac{d^2Y^\circ}{d\zeta^2} + \left[\frac{1}{2}\left(\frac{1}{\zeta} + \frac{1}{\zeta-1} + \frac{1}{\zeta-1/k^2}\right) - \frac{1}{\zeta-f_0}\right]\frac{dY^\circ}{d\zeta} + \frac{\mu\zeta+\lambda}{4\zeta(\zeta-1)(k^2\zeta-1)(\zeta-f_0)}Y^\circ = 0 \tag{2.4}$$

where μ and λ are unknown auxilliary parameters. We assume that two particular, linearly independent solutions Y_1° and Y_2° of (2.4) have been found; then, taking into account (2.1) we can write

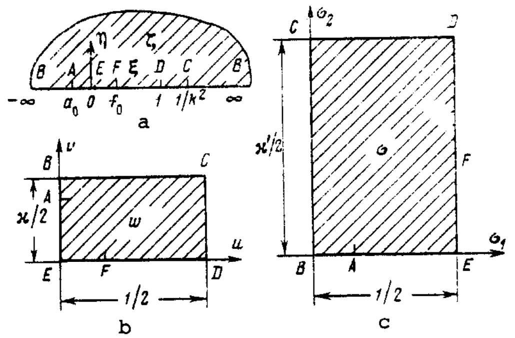

Fig.3

$$W = W_x - iW_y = \frac{d\omega}{dz} = \frac{\Omega}{Z} = \frac{\Omega^\circ}{Z^\circ}; \tag{2.5}$$
$$\Omega^\circ = c_1 Y_1{}^\circ + c_2 Y_2{}^\circ, \quad Z^\circ = c_3 Y_1{}^\circ + c_4 Y_2{}^\circ$$

Functions Z°, Ω° are connected with the functions Z and Ω by (2.3), and $c_1, \ldots, c_4$ are certain constants. Using the substitution

$$\zeta = \mathrm{sn}^2(2Kw, k) \tag{2.6}$$

we map the half-space $\operatorname{Im}\zeta \geqslant 0$ onto a rectangle (Fig.3b), whereupon (2.4) becomes

$$\frac{d^2Y^\circ}{dw^2} - 2\Delta_0^{-1}\,\mathrm{sn}(2Kw, k)\,\mathrm{cn}(2Kw, k)\,dn(2Kw, k)\frac{dY^\circ}{dw} + \tag{2.7}$$
$$\Delta_0^{-1}[\mu\,\mathrm{sn}^2(2Kw, k) + \lambda] = 0; \ \Delta_0 = \mathrm{sn}^2(2Kw, k) - \mathrm{sn}^2(2Kw_0, k)$$

Here sn, cn, dn are analytic Jacobi functions, K is the total elliptic integral of first kind with modulus k /6,7/, the latter unknown just as the coordinate w_0 of the point F in the w-plane connected with the parameter f_0 by (2.6).

In view of the similarity between (2.7) and the Lamé equation we shall take, following /8/, the functions $Y_{1,2}{}^\circ$ in the form

$$Y_{1,2}^\circ = \frac{\vartheta_4(w \pm \alpha, \varkappa)}{\vartheta_4(w, \varkappa)}; \quad \varkappa = \frac{K'}{K}, \quad K' = K(k'), \quad k' = \sqrt{1 - k^2} \tag{2.8}$$

We shall retain the notation used in /7/ for ϑ_4 and other theta functions.

Substituting (2.8) into (2.5) we obtain for $W(w)$ the representation in which the real parameter α and the ratios of three of the constants $c_1, \ldots, c_4$ to the fourth constant different from zero, are all unknown. To find them we use the correspondence of the corner points of the regions w and W, and the fact that the segment ED lies in the plane W of the circumference $|W + i\rho/2| = \rho^2/4$. As a result we obtain

$$c_{1,\ldots,4} = A\overset{\circ}{c}_{1,\ldots,4}; \quad c_{1,2}{}^\circ = \pm\rho\sin\pi\beta, \quad c_{3,4}{}^\circ = e^{\pm i\pi\beta} \tag{2.9}$$
$$\alpha = \frac{1}{\pi}\operatorname{arctg}\sqrt{\frac{\varepsilon(1+\rho)}{\rho - \varepsilon}}, \quad \beta = -\frac{1}{\pi}\operatorname{arctg}\sqrt{\frac{\varepsilon}{(\rho-\varepsilon)(1+\rho)}}$$

Using direct substitution and the properties of theta functions /7/ we can establish that the function $\overline{W}(w)$ given by (2.5),(2.8) and (2.9), maps the rectangle w onto the velocity hodograph $\overline{W}$. The functions $Z^\circ(w), \Omega^\circ(w)$ are also determined with the accuracy of up to a constant. Considering further dz/dw and $d\omega/dw$, as unknown functions we obtain, by virtue of (2.1), (2.3) and (2.6),

$$Y(w) = Y(\zeta)\,d\zeta/dw = Y^\circ(w)/\sqrt{\Delta_A} \tag{2.10}$$
$$\Delta_A = \mathrm{sn}^2(2Kw, k) - \mathrm{sn}^2(2Kw_A, k)$$

where $\overline{Y}(w)$ is the general integral of the equation satisfied by the above functions, The relations (2.5) and (2.8)–(2.10) lead to

$$\frac{dz}{dw} = A\,\frac{e^{i\pi\beta}\vartheta_4(w - \alpha, \varkappa) + e^{-i\pi\beta}\vartheta_4(w + \alpha, \varkappa)}{\vartheta_4(w, \varkappa)\sqrt{\Delta_A}} \tag{2.11}$$
$$\frac{d\omega}{dw} = A\rho\sin\pi\beta\,\frac{\vartheta_4(w - \alpha, \varkappa) - \vartheta_4(w + \alpha, \varkappa)}{\vartheta_4(w, \varkappa)\sqrt{\Delta_A}}$$

It can be shown that the functions (2.1) determined from (2.11) and (2.6) satisfy the boundary conditions (1.1) written in terms of the above functions, and represent therefore a parametric solution of the initial boundary value problem. We further find

$$W(w) = \frac{d\omega}{dz} = \rho\sin\pi\beta\,\frac{\vartheta_4(w - \alpha, \varkappa) - \vartheta_4(w + \alpha, \varkappa)}{e^{i\pi\beta}\vartheta_4(w - \alpha, \varkappa) + e^{-i\pi\beta}\vartheta_4(w + \alpha, \varkappa)} \tag{2.12}$$

The coordinate w_0 of the point of inflection F of the line of separation ED (Fig.1) satisfies the following equation resulting from the relation $W'(w_0) = 0$ (Fig.2,3), (2.12) and known /8,9/ relations connecting the function ϑ_4 with the Jacobi zeta function $Z(u)$:

$$Z[2K(w_0 - \alpha)] - Z[2K(w_0 + \alpha)] = 0 \tag{2.13}$$

Using the properties of zeta functions /9/ we can show that equation (2.13) has, at any value of $\alpha \in (0, {}^1/_2)$, a unique solution $w_0 \in (0, {}^1/_2)$. Since the function (2.8) satisfies the equation (2.7), its left-hand side should become identically zero in the rectangle w (Fig.3b) after substituting into it the above functions, and by virtue of its double periodicity, also in the whole w-plane. This leads, after the relevant transformations, to the following system of equations in terms of the parameters w_0, μ and λ:

$$\begin{gathered}\lambda = [Z^2(2\alpha K) - k^2 \operatorname{sn}^2(2\alpha K, k)] \operatorname{sn}^2(2Kw_0, k) \\ \mu \operatorname{sn}^2(2Kw_0, k) + \lambda = 2 \operatorname{sn}(2Kw_0, k) \operatorname{cn}(2Kw_0 k) \times \\ \operatorname{dn}(2Kw_0, k) \ \{Z[2K(w_0 + \alpha)] - Z(2Kw_0)\}\end{gathered} \tag{2.14}$$

We note that equation (2.13) follows from the second and third equation of (2.14). Taking all we said into account, we conclude that the parameters w_0, μ and λ can be determined uniquely from the system (2.14) at any value of $\alpha \in (0, {}^1/_2)$.

Let us note two limit cases related to the degeneration of the velocity hodograph. *1)* $\varepsilon = 0$. According to (2.9), (2.12) and (2.11) we have $\alpha = \beta = 0$, $\overline{W}(w) \equiv 0$, and the region z transforms into a rectangle. In the absence of evaporation of the stagnant water the fresh water fills the whole layer of soil between two horizontal planes, i.e. the surface soil and the surface of the saline ground water.

2) $l = L$ merger of the channels. Points B and C merge (Fig.1) and the rectangle w becomes a half-strip (Fig.3b). We also have $k = 0$, $\vartheta_4(w \pm \alpha, \varkappa) \equiv 1$, and by virtue of (2.12) we obtain $\overline{W}(w) \equiv 0$.

In practice, the distance between the channels is much greater, as a rule, than the depth of the bed of saline ground water and the width of the channel. Computations based on the first equation of (2.11) show that a similar relation between the geometrical parameters of the border is ensured if $k \approx 1$, but in this case the representation (2.11) itself becomes invariant since the convergence of the series in the theta functions is weakened. It is expedient therefore to transform the latter to theta functions using an auxilliary modulus k'. The transformation $\sigma = {}^1/_2 + iw\varkappa_1$, $\varkappa_1 = \varkappa^{-1} = K/K'$ reduces the first equation of (2.11) to the form

$$\begin{gathered}\frac{dz}{d\sigma} = C\frac{e^{i\pi(\gamma - 2\alpha\sigma)}\vartheta_1(\sigma - i\alpha\varkappa_1, \varkappa_1) + e^{-i\pi(\gamma-2\alpha\sigma)}\vartheta_1(\sigma + i\alpha\varkappa_1, \varkappa_1)}{\sqrt{a^2 - \operatorname{sn}^2(2K'\sigma, k')}\,\vartheta_4(\sigma, \varkappa_1)} \\ \gamma = \alpha + \beta, \ a = \operatorname{sn}(2K\sigma_A, k')\end{gathered} \tag{2.15}$$

When $k' = 0$, we have $\varkappa_1 = \infty$; region σ (Fig.3c) degenerates into a half-strip $\{0 \leqslant \sigma_1 \leqslant {}^1/_2, \sigma_2 \geqslant 0\}$, and the border into a chain of equal lenses each of which is connected to the adjacent lenses at the corner points. Carrying out in (2.15) a passage to the limit with $k' \to 0$ we arrive, as a result, at the relation

$$\frac{dz}{d\sigma} = C_1\frac{m \sin(\delta\pi\sigma) + \cos(\delta\pi\sigma)}{\sqrt{a^2 - \sin^2(\pi\sigma)}}, \quad m = \operatorname{ctg}\pi\gamma, \quad \delta = 1 - 2\alpha$$

obtained earlier for the problem of the lens at $\varepsilon < \rho$ /1/. We note that the solution itself, constructed for this case, and the filtration scheme in the lens described by this solution, exhaust themselves at $\varepsilon = \rho$, since a constraint $|W| \leqslant \rho$, exists at the line of separation governed by the assumption that the saline waters are stagnant. When $\varepsilon > \rho$, the segments corresponding in the W-plane to the depression curve and the line of separation no longer intersect, and an additional segment must be brought in to close the boundary of the velocity hodograph. Within this segement, the rate of filtration is reduced to the limiting value of ρ admissible at the boundary line. Thus the passage to the case $\varepsilon > \rho$ is accompanied by a rearrangement of the flow pattern.

A different pattern is obtained in the case of the border zone. Carrying out the passage to the limit $\varepsilon \to \rho$ in (2.12), using the formulas (2.9) for α and β, and using the L'Hospital rule to evaluate the indeterminacy 0/0 we find, after some manipulation,

$$W(w)|_{\varepsilon=\rho} = \rho\frac{2KZ[K(2w-1)]}{-\pi(1+\rho) + i2KZ[K(2w-1)]} \tag{2.16}$$

We can obtain the same expression by inversion of the region $\overline{W}$ relative to the circle with the center at the point $\overline{W} = i\varepsilon$, which, in the present case, represents the point of intersection of all boundary segments of the hodograph.

The mapping (2.16) determines, as expected, the hodograph of the same construction (Fig. 2) as the mapping (2.12). At the point D where $w = {}^1/_2$ we have $W = 0$, and the tangent to the line of separation is horizontal as in the case $\varepsilon < \rho$. The initial flow pattern within the border remains in force, due to the presence of the segment CD between the depression curve and line of separation. Its amortizing action is apparently retained together with the filtration scheme, and, when the parameter ε increases over the certain interval (ρ, ε^*). Further, we can expect the appearance of a critical regime similar to those observed in other hydrodynamic models of the border /10–12/, with a half-circle $|\overline{W} - i\rho/2| \leqslant \rho^2/4$ becoming separated from the region of the hodograph (Fig.2) and the point D on the line of separation converted into a cusp. The above problems however require special analysis based on the solution of the case $\varepsilon > \rho$.

Let us note that the limiting case $\rho = \infty\ (\rho_2 = \infty)$, which can be treated, within the framework of the filtration scheme under consideration, as "solidification" of the saline water. The line of separation is transformed into a horizontal water confining stratum, and it can easily be confirmed by using the equation (2.12) with help of (2.9) for β, and taking into account the fact that $\psi = 0$ on ED. As a result we obtain, for $\rho = \infty$,

$$\frac{1}{W_{ED}} = \left(\frac{dz}{d\varphi}\right)_{ED} = \frac{1}{\sqrt{\varepsilon}} \cdot \frac{\vartheta_4(w-\alpha,\varkappa) + \vartheta_4(w+\alpha,\varkappa)}{\vartheta_4(w-\alpha,\varkappa) - \vartheta_4(w+\alpha,\varkappa)};$$
$$0 \leqslant w \leqslant {}^1/_2$$
$$\alpha = \frac{1}{\pi}\operatorname{arctg}\sqrt{\varepsilon}$$

and therefore we have $(\partial y/\partial\varphi)_{ED} = 0$, $y_{ED} = \text{const}$.

3. Computational scheme and analysis of the results. Writing the representation (2.15) for various segments of the boundary of σ, followed by integration, yields the parametric equations of the corresponding boundary segments of the border, containing three unknown constants, namely C, a and k'. Assuming, as stated in Sect.1, that the quantities l, L and H_0 included in the set of defining parameters are known, we obtain the following system of equations:

$$F_1(C,a,k') = \int_0^{\sigma_A} X_{AB}(\sigma)\,d\sigma = l; \qquad \sigma_A = \frac{1}{2K'}F(\arcsin a, k') \tag{3.1}$$

$$F_2(a,k') = f_2[a,k',C(a,k')] = \int_{1/2}^{(1+i\varkappa_1)/2} X_{ED}(\sigma)\,d\sigma = L$$

$$F_3(k') = f_3[k', a(k')] = \frac{1}{L}\int_{1/2}^{(1+i\varkappa_1)/2} y_{ED}(\sigma)\frac{dx_{ED}(\sigma)}{d\sigma}\,d\sigma =$$

$$\frac{1}{L}\int_{1/2}^{(1+i\varkappa_1)/2} X_{ED}(\sigma)\left[\int_{1/2}^{\sigma} Y_{FD}(\tau)\,d\tau\right]d\sigma = H_0;$$

$$X = \operatorname{Re}\left(\frac{dz}{d\sigma}\right), \qquad Y = \operatorname{Im}\left(\frac{dz}{d\sigma}\right)$$

where $F(\varphi, k')$ is an elliptic integral of first kind in the normal Legendre form. The left hand part of the last equation, identical to (1.3), is written as an implicit function of the parameter k'. The parameter $a(k')$ appearing in it can be found from the second equation of (3.1) from which the constant $C(a, k')$ has been previously eliminated with help of the first equation.

Computations show that when the parameter $k' \in (0, 1)$ is fixed, the function $F_2(a, k')$ decreases monotonously in a while the latter increases over the interval $(0, 1)$, and $F_2(0, k') = \infty$, $F_2(a, k') \to l$ as $a \to 1$. Thus when $L > l$, the parameter a is given uniquely by the second equation of (3.1). The function $F_3(k')$ is found to be (also according to the computations) monotonously increasing over the interval (H_{00}, ∞). The value $H_{00} = F_3(0)$ corresponds to the limiting case mentioned above (when the border is transformed into a chain of lenses) and is found, in each concrete case, for the formula

$$H_{00} = \frac{1}{L}\int_0^L \mathring{y}_{ED}(x)\,dx \tag{3.2}$$

Here $\mathring{y}_{ED}(x)$ is the ordinate of the boundary line for the lens, computed with help of the analytical solution obtained earlier in /1/, using the parameters l and L adopted for the border.

Computing over the border is carried out in the case $H_0 > H_{00}$ where (3.1) are used, as before, to determine the constants C, a and k', and this is followed by finding the coordinates of the points on the depression curve BC and the boundary line ED. We also find, at every point of the depression curve computed, the evaporation intensity ε_s /1/, for which we have in accordance with (1.1),

$$\varepsilon_s = \left|\frac{\partial\psi}{\partial s}\right| = \varepsilon \frac{\partial x}{\partial s}\bigg|_{BC} = \varepsilon\,[1 + (dy/dx)^2_{BC}]^{-1/2}$$

The second and third equation of (3.1) are solved using the method of half division and linear interpolation. The number of terms in the theta function series in all formulas is set by the program so as to obtain the prescribed computational accuracy. Integration of the equation (2.15) over the whole contour of the region σ within which the function $z(\sigma)$ is analytic, serves as control of the computations.

Initial parameters	Lens			Border zone $H_0=30$				Border zone $H_0=15$			
	H	$10^3 \cdot T$	H_{co}	$10^3 \cdot k$	H_1	H_2	$10^3 \cdot T$	$10^4 \cdot k$	H_1	H_2	$10^3 \cdot T$
	14.16	224	8.187	283	31.04	29.05	137	179	18.14	12.27	157
$l=0.5$	14.19	248	8.212	282	31.04	29.05	161	177	18.15	12.26	180
5	13.88	171	8,088	293	31.00	29.07	84	202	18.02	12.23	103
10	13.17	144	7,906	320	30.92	29.13	61	273	17.69	12.46	78
$L=25$	7,053	101	4.079	830	30.07	29.93	55	2846	15.52	14.53	57
100	28.37	496	16.42	18	36.31	24.52	361	Border zone $H_0=10$			
$10^3 \cdot \rho=2$	28.15	156	18.68	264	34.61	25.55	137	4	14.92	5.243	186
50	6.883	391	3.849	284	30.21	29.81	137	204	15.70	14,48	157
∞		1.577		284	30,00		137	205	15.00		157
$10^4 \cdot \varepsilon=1$	4.815	53	2,544	286	30.11	29.91	14	213	15.35	14,75	16
5	10,31	140	5.738	285	30.53	29.53	68	203	16.67	13,69	78
30	23.01	522	14.57	271	32.95	26.92	420	9	23.14	3.289	500
50	28.64	811	19,24	250	34.73	24.37	719	Border zone $H_0=20$			
90	36.69	1429	26.78	166	38.09	16.36	1382	749	22.12	18.15	145

The above table gives the results of computations for the characteristic dimensions of the border zone at $H_0 = 30$ and 15. Both series contain four groups of variants, in each of which only one of the parameters l, L, ρ and ε varies, with the remaining parameters fixed at the values $l = 1$; $L = 50$; $\rho = 0.01$; $\varepsilon = 0.001$ (the linear quantities can be assigned any dimension of length). The variants with such a combination appear in the first line of the table, enter as pivotal all groups of variants where the lines in the table are interrupted, and form themselves a group with respect to the parameter H_0 together with the variants of the border zone at $H_0 = 10$ and 20. The latter are situated in the empty spaces in the table, appearing in the series $H_0 = 15$, for the four combinations at which border zone does not exist since $H_{00} > 15$. Three cases of decomposition of the border zone into a chain of lenses shown in the table are connected with the influence of such factors as increased distance between the channels, more intense evaporation and reduction in density of the saline water. The group of variants with respect to parameter ρ is terminated by the limit scheme with a dam mentioned above.

The table also gives, for every variant of the border zone, the values of the parameter k' most sensitive to the relation between the width of the border zone $2L$ and its mean depth H_0. Let us pause at the variants $H_0 = 15; l = 0.5; L = 50$ and $H_0 = 30; l = 1; L = 100$ (the second and sixth line). Here the characteristic dimensions of the border zone and the lens also differ from each other by a factor of two. In (2.16) such a difference is related only to the coefficient C with the accuracy of up to which the system (3.1) remains the same for both variants compared here. For this reason the value of the parameter k' will also remain the same.

Reducing the magnitude of l at fixed values of L and ε is accompanied, within the restrictions imposed by (1.2), by the increase in the length $L - l$ of the depression curve and total evaporation from it $\varepsilon(L - l)$ equal to the filtration flow from the channel, therefore the mean filtration rate $\varepsilon(L - l)/l$ through the bottom of the channel is also increased. Similar strengthening of the flow at the entry to the border zone intensifies the effect of displacement of the boundary line manifesting itself by the increase in H_1. The change in the width of the channel affects, to even a greater extent, the depression curve. The evaporation intensity ε affects analogously the position of the movable boundaries. In contrast, the variation in the parameter ρ affects insignificantly the depression curve of the border zone, but deforms appreciably the dividing line.

In the case of several computational variants, a slight increase in the value of H_0 over its limit admissible value (in the border zone scheme) H_{00} shows the corresponding characteristic sizes of the border zone and the lens to be close to each other, and the parameter k' in these cases is small. It also diminishes appreciably in the case when $L = 100$, although there are no explicit indications of decomposition of the border zone into lenses. The width of the neck CD (Fig.1) remains in this case considerable. Comparing the values of the parameter k' in the three variants of the group relative to L for $H_0 = 30$, reflects its sensitivity mentioned above to the ratio of the length of the flow region to its mean depth.

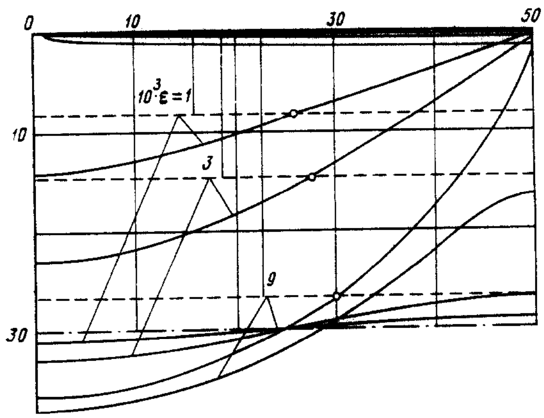

Fig.4

Fig.4 depicts three variants of the table from the group related to parameter for the value $H_0 = 30$. The mean values of the depth H_{00} of the corresponding lenses are shown with dashed lines. The depression curves for the border zone and the lens are close to each other in each of the three variants, and are depicted in the figure by a single line.

The authors express due gratitude to N.S. Kolodei for assistance in carrying out the computations.

REFERENCES

1. POLUBARINOVA-KOCHINA P.Ia., PRIAZHINSKAIA V.G. and EMIKH V.N., Mathematical Methods in Irigation Problems. Moscow, NAUKA, 1969.
2. KAPRANOV Iu.I., The form of fresh-water lens for linear evaporation law. PMM Vol.37, No.3, 1973.
3. POLUBARINOVA-KOCHINA P.Ia., Theory of Motion of Ground Water. Moscow, NAUKA, 1977.
4. ARAVIN V.I. and NUMEROV S.N., Theory of Motion of Liquids and Gases in Undeformable Porous Medium. GOSTEKHIZDAT, Moscow, 1953.
5. GOLUBEV V.V., Lectures on Analytic Theory of Linear Differential Equations. Moscow-Leningrad, GOSTEKHTEORIZDAT, 1950.
6. GRADSHTEIN I.S. and RYZHIK I.M., Tables of Integrals, Sums, Series and Products, Moscow, Fizmatgiz, 1962.
7. JAHNKE E., EMDE F., and LÖSCH F., Tables of Functions with Formulae and Curves. N.Y. Dover Publ. 1945.
8. WHITTAKER E.T. and WATSON G.N., A course of Modern Analysis Pt.2, Cambridge Univ. Press, 1940.
9. BYRD P.F. and FRIEDMAN M.D., Handbook of elliptic integrals for engineers and scientists. B. Springer, 1971.
10. KAPRANOV Iu.I., Fresh-water lens produced by uniform filtration. PMM Vol.38, No.6, 1974.
11. KAPRANOV Iu.I., On the border zone of fresh water in the case of a periodic system of horizontal drainage pipes. In: Boundary Value Problems of Underground Hydrodynamics. Kiev. Izd-c In-ta matem. Akad. Nauk UkrSSR, 1975.
12. EMIKH V.N., Hydrodynamic model of drainage in the border zone of subsoil fresh water lying above saline water. Dokl. Akad. Nauk SSSR, Vol. 252, No.4, 1980.

Translated by L.K.